Interannual variations in degree-2 Earth's gravity coefficients C-2,C-0, C-2,C-2, and S-2,S-2 reveal large-scale mass transfers of climatic origin

B. Meyssignac, J. M. Lemoine, Gm. Chen, A. Cazenave, P. Gegout, Philippe Maisongrande

Interannual variations in degree-2 Earth's gravity coefficients $C_{2,0}$, $C_{2,2}$, and $S_{2,2}$ reveal large-scale mass transfers of climatic origin

B. Meyssignac,[1,2] J. M. Lemoine,[1,3] M. Cheng,[4] A. Cazenave,[1,2] P. Gégout,[1,5] and P. Maisongrande[1,2]

Received 25 June 2013; accepted 13 July 2013.

[1] Several recent studies have shown evidences for large water transfers in the climate system at interannual to decadal time scales, in particular during El Niño-Southern Oscillation events. In this study, we investigate further these water transfers and their signature in the gravity field. We analyze variations of the low-degree spherical harmonics $C_{2,0}$ (Earth's oblateness), $C_{2,2}$, and $S_{2,2}$ (eccentricity at the Earth's equator) from satellite laser ranging data during the 19 year period 1993–2012. We also estimate the water mass transfers in the climate system using satellite altimetry corrected for the steric effect, atmospheric reanalysis, and land hydrology models. We find a large signal in the water mass redistribution during the 1997/1998 El Niño which is consistent with an increase of the ocean mass in the tropical Pacific, a decrease of water storage in the Amazon Basin, and an increase of water storage in the Congo Basin.
Citation: Meyssignac, B., J. M. Lemoine, M. Cheng, A. Cazenave, P. Gégout, and P. Maisongrande (2013), Interannual variations in degree-2 Earth's gravity coefficients $C_{2,0}$, $C_{2,2}$, and $S_{2,2}$ reveal large-scale mass transfers of climatic origin, *Geophys. Res. Lett.*, *40*, doi:10.1002/grl.50772.

1. Introduction

[2] *Llovel et al*. [2011] and *Boening et al*. [2012] showed that interannual global mean sea level (GMSL) and total land water storage variations are inversely correlated, in particular during El Niño-Southern Oscillation (ENSO) events. Total water storage is lower/higher than average on land when GMSL is higher/lower than average during El Niño/La Niña. This result is in agreement with the observed rainfall deficit/excess over land/oceans during El Niño and vice versa during La Niña [*Gu and Adler*, 2011]. It suggests that the GMSL anomalies observed during ENSO events are likely due to an ocean mass excess rather than thermal expansion increase. In a recent study which focuses on the large positive GMSL anomaly observed during the 1997/1998 El Niño, *Cazenave et al*. [2012] showed that this anomaly is almost exclusively due to an ocean mass excess located in the north tropical Pacific. At the same time, they observe a total land mass deficit (essentially located within the tropics) that is equivalent in amplitude and phasing to the ocean mass excess observed in the north tropical Pacific. These results suggest that the main modes of interannual climate variability (in particular ENSO) generate large mass redistributions (essentially water) over the globe between remote places.

[3] In this study, we investigate further these large-scale water mass redistributions and their signature in the gravity field. We analyze interannual variations of the degree-2 spherical harmonics measured by satellite laser ranging (SLR, Pearlman et al., 2002) during a 19 year period (1993–2012) which encompasses the intense 1997/1998 El Niño. The mass transfer observed by *Cazenave et al*. [2012] during the 1997/1998 El Niño is essentially longitudinal and occurs between land and ocean, within the tropics. So we mainly focus here on the degree-2 order-2 spherical harmonic of the gravity field ($C_{2,2}$ and $S_{2,2}$), which is related to the eccentricity at the Earth's equator and reveals longitudinal mass transfers. This analysis of $C_{2,2}$ and $S_{2,2}$ interannual variability is original in the literature and brings new insights into mass redistributions of climatic origin at the Earth's surface. We also analyze latitudinal mass transfers over the whole period (1993–2012) with the degree-2 order-0 spherical harmonic of the gravity field ($C_{2,0}$), which is related to the Earth's oblateness and indicates mass transfers between high (>35.3°) and low (<35.3°) latitudes. By accounting for water mass redistribution in ocean and land with independent observations (including satellite altimetry and in situ hydrographic measurements) and models (land hydrology models), we are able to explain the interannual variability in large-scale mass redistribution observed since 1993 with the $C_{2,0}$, $C_{2,2}$, and $S_{2,2}$ variations corrected for the atmospheric effects. Section 2 explains the determination of $C_{2,0}$, $C_{2,2}$, and $S_{2,2}$ time series (corrected for the atmospheric effect) from SLR tracking data, on the one hand, and from water mass redistribution in ocean and land, on the other hand. In section 3, we compare both estimations of $C_{2,0}$, $C_{2,2}$, and $S_{2,2}$ and we analyze the role played by ocean and land mass redistributions in their variations. We show that during the 1997/1998 El Niño, some large mass transfers occurred at the Earth's surface from the extratropics to the tropics and also within the tropics between ocean and land. These mass transfers explain the variations observed in $C_{2,0}$, $C_{2,2}$, and $S_{2,2}$ coefficients by SLR tracking between January 1997 and December 1998.

2. Data and Methodology

[4] We compare the $C_{2,0}$, $C_{2,2}$, and $S_{2,2}$ time series over 1993–2012 computed from SLR data corrected for atmospheric effects with independent estimates based

[1]Université de Toulouse/UPS (OMP-PCA), Toulouse, France.
[2]CNES/LEGOS, Toulouse, France.
[3]CNES/GET, Toulouse, France.
[4]CSR, Austin, Texas, USA.
[5]CNRS/GET, Toulouse, France.

Corresponding author: B. Meyssignac, Université de Toulouse/UPS (OMP-PCA), 14 Av. Edouard Belin, FR-31400 Toulouse, France. (benoit.meyssignac@legos.obs-mip.fr)

0094-8276/13/10.1002/grl.50772

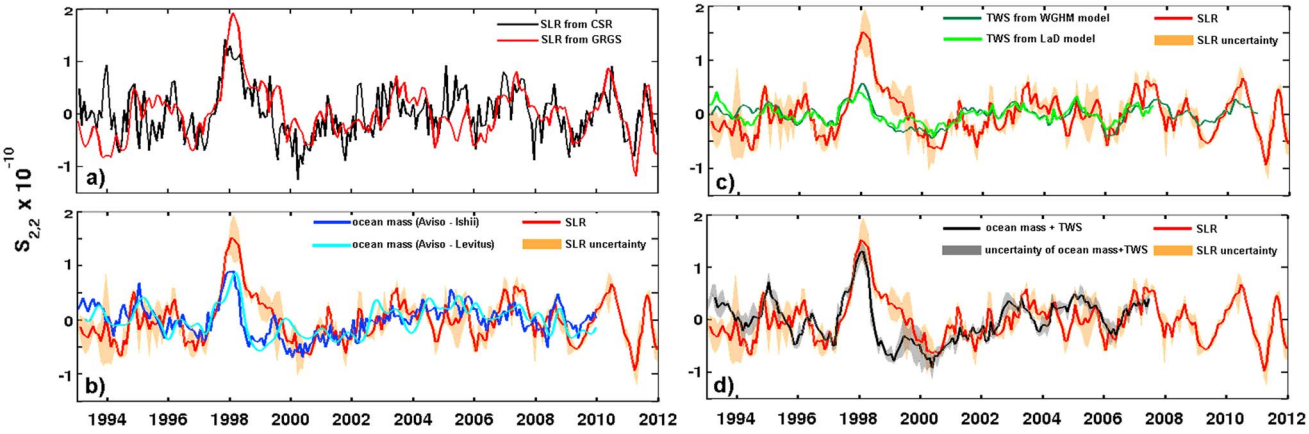

Figure 1. (a) S_{22} variations from SLR data computed by GRGS (red curve) and CSR (black curve). (b–d) S_{22} variations from SLR data (mean of CSR and GRGS solutions) are in red with uncertainty (orange shaded area). The ocean mass contribution is plotted on Figure 1b with estimations based on data from *Levitus et al*. [2012] (light blue curve) and from *Ishii and Kimoto* [2009] (dark blue curve). The land mass contribution is plotted on Figure 1c with estimations based on the LaD model (light green curve) and on the WGHM model (dark green curve). The sum of the ocean and land mass contributions is plotted on Figure 1d (black curve) with uncertainty (grey shaded area).

on the spherical harmonic decomposition of ocean mass redistribution deduced from altimetry corrected for steric effect and total land water storage obtained from global hydrology models.

2.1. $C_{2,0}$, $C_{2,2}$, and $S_{2,2}$ Variations From SLR Data

[5] SLR-observed solutions for $C_{2,0}$, $C_{2,2}$, and $S_{2,2}$ variations are obtained from two different research groups: the Groupe de Recherches de Géodésie Spatiale (GRGS) and the Center for Space Research (CSR). The CSR solution is based on the methodology described by *Cheng et al*. [2013]. It is computed with data from eight satellites (LAGEOS-1 and 2, Etalon-1 and 2, Starlette, Stella, Ajisai, and BEC). The GRGS solution is based on data from LAGEOS-1 and 2 only. Both CSR and GRGS used the updated models of the IERS2010 convention, the ocean pole tide from *Desai* [2002], and the FES2004 ocean tides from *Lyard et al*. [2006] in their processing. CSR used the EGM2008 gravity model from *Pavlis et al*. [2012], and GRGS used the EIGEN-GL04S gravity model from *Forste et al*. [2008]. Both solutions of CSR and GRGS are corrected for the atmospheric effects with the surface pressure data from the ECMWF (European Centre for Medium-Range Weather Forecasts) operational analyses.

[6] In this paper we focus on the interannual variability of $C_{2,0}$, $C_{2,2}$, and $S_{2,2}$ variations. So trends over the study period (1993–2012) are removed. By detrending time series, we remove from $C_{2,0}$, $C_{2,2}$, and $S_{2,2}$ any secular time scale signals such as the glacial-isostatic adjustment effect associated to the last deglaciation [*Roy and Peltier*, 2011; *Nerem and Wahr*, 2011]. By detrending, we also remove multidecadal signals due to climate processes such as the present-day ice mass loss in Greenland and Antarctica (the signal of this ice mass loss impacts essentially the trend of the low-degree spherical harmonics time series over the past two decades [see *Nerem and Wahr*, 2011]), part of the signal from the current melting of glaciers [*Dickey et al*., 2002; *Cheng et al*., 2013], and potentially some long-term land, atmosphere, and ocean mass redistributions. However, all the interannual to decadal signal, which is essentially of climatic origin, is retained in the detrended time series of $C_{2,0}$, $C_{2,2}$, and $S_{2,2}$ [*Chao et al*., 2003; *Cheng et al*., 2013].

2.2. $C_{2,0}$, $C_{2,2}$, and $S_{2,2}$ Variations From Ocean Mass Redistribution and Land Water Storage

[7] We compute the contribution of land and ocean interannual mass redistributions on $C_{2,0}$, $C_{2,2}$, and $S_{2,2}$ by expressing them in spherical harmonics.

[8] Ocean mass redistributions are estimated by correcting the sea level signal for the steric effect. Sea level data are retrieved from AVISO (Archiving, Validation, and Interpretation of Satellite Oceanographic data, http://www.aviso.oceanobs.com/en/data/products/sea-surface-height-products/global/msla/index.html). We used the merged satellite product (namely DT-MSLA "Ref" series) based on several altimetry missions (Topex/Poseidon, Jason-1 and 2, Envisat, ERS-1 and 2) which covers the period 1993–2011 with a one-fourth degree resolution on a weekly basis. This sea level data set is already corrected for the inverse barometer effect with the ECMWF operational analyses (which is consistent with the atmospheric correction applied to the SLR time series of $C_{2,0}$, $S_{2,2}$, and $C_{2,2}$). We subsampled the sea level data set at 1° resolution and monthly interval to correct it for the steric effect. The steric effect was computed by integrating the water columns density changes down to 700 m depth with the temperature and salinity data sets of *Ishii and Kimoto* [2009] and *Levitus et al*. [2012]. The sea level data set from AVISO does not cover the northern part of the Arctic region (>82° latitude), and the steric computation does not take into account the deep ocean (deeper than 700 m). So the resulting ocean mass redistribution estimate, which is computed as the difference between sea level and steric sea level, does not include the latter two contributions. But we expect them to be small. (Estimates of the ocean mass from Gravity Recovery and Climate Experiment (GRACE) satellites over 2003–2012 show that the ocean mass signal in the Arctic region, above 82°N, is indeed very small. It represents less than 3.6% of the variance of the global ocean mass signal at interannual

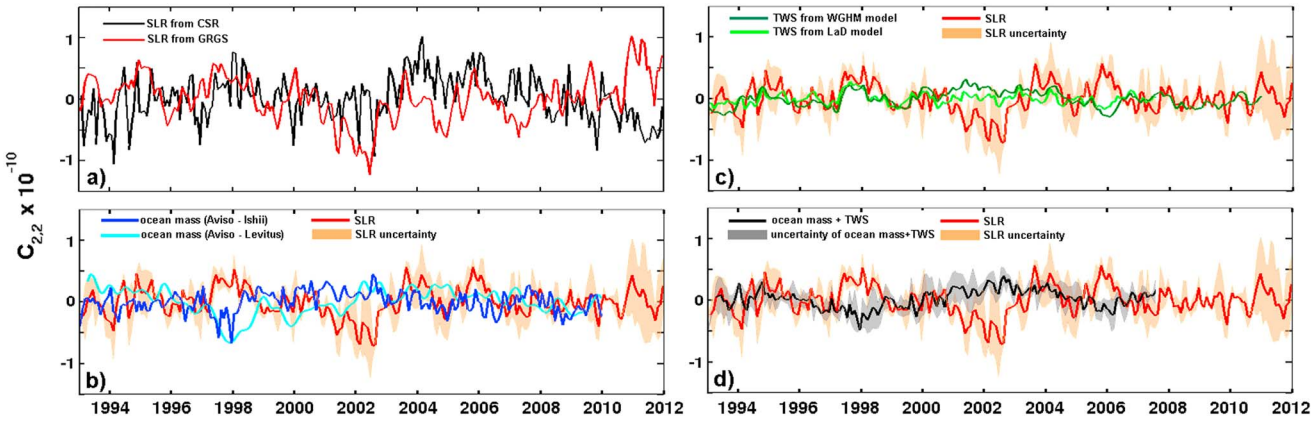

Figure 2. (a) C_{22} variations from SLR data computed by GRGS (red curve) and CSR (black curve). (b–d) C_{22} variations from SLR data (mean of CSR and GRGS solutions) are in red with uncertainty (orange shaded area). The ocean mass contribution is plotted on Figure 2b with estimations based on data from *Levitus et al*. [2012] (light blue curve) and from *Ishii and Kimoto* [2009] (dark blue curve). The land mass contribution is plotted on Figure 2c with estimations based on the LaD model (light green curve) and on the WGHM model (dark green curve). The sum of the ocean and land mass contributions is plotted on Figure 2d (black curve) with uncertainty (grey shaded area).

time scales.) Another source of error in our estimate of the ocean mass redistribution comes from the sparse temperature and salinity data used for the steric correction (particularly sparse before the Argo era, i.e., before 2004). To evaluate the uncertainty due to these sparse data, we compared here two temperature and salinity data sets: (1) *Ishii and Kimoto* [2009] and (2) *Levitus et al*. [2012]. Both data sets are based on the same sparse measurements, but they use different numerical schemes to fill in the gaps (in time and space) where temperature and salinity data are missing. Discrepancies in ocean mass redistribution (and subsequent ocean contribution to $C_{2,0}$, $C_{2,2}$, and $S_{2,2}$; see Figures 1b, 2b, and 3b) between estimates based on *Ishii and Kimoto* [2009] data set and *Levitus et al*. [2012] data set provides an estimate of the uncertainty due to the filling method.

[9] Land water storage is estimated with monthly gridded outputs of two land surface models: (1) the WaterGap Global Hydrology Model (WGHM) [*Doll et al*., 2003] and (2) the Land Dynamics (LaD) model [*Milly and Shmakin*, 2002]. WGHM outputs are available through December 2009, and LaD outputs are available through July 2007. When available, Greenland and Antarctica data are removed because hydrological models do not provide the ice mass balance contribution. At global scale, WGHM and LaD show differences in their land water storage estimation due to different numerical schemes and different meteorological forcings. These differences provide an estimate of the model uncertainties [*Syed et al*., 2009]. Note that data from the space gravimetric mission GRACE could also be used in this study, but the GRACE data start only in 2002.

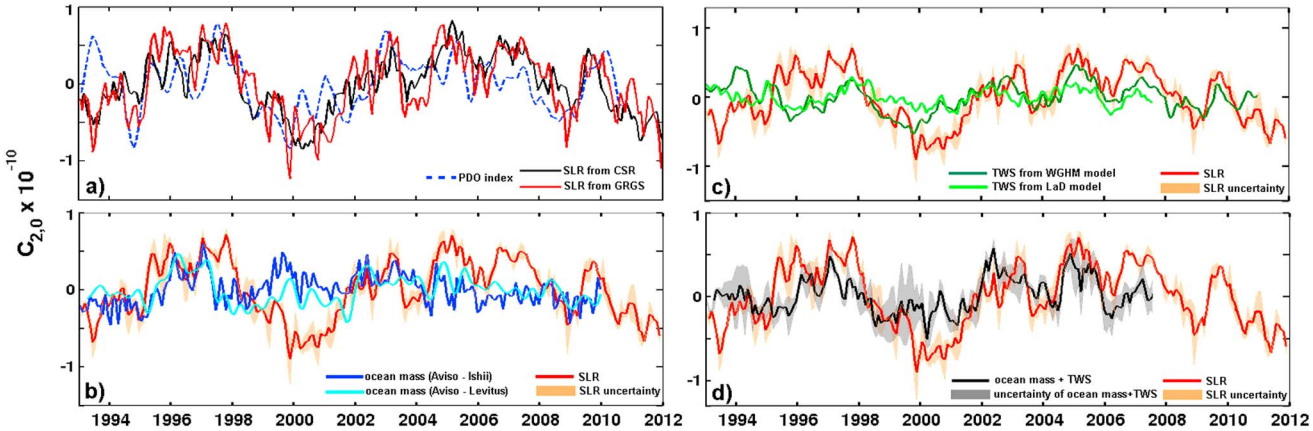

Figure 3. (a) C_{20} variations from SLR data computed by GRGS (red curve) and CSR (black curve) against the normalized PDO index (blue dashed curve). (b–d) C_{20} variations from SLR data (mean of CSR and GRGS solutions) are in red with uncertainty (orange shaded area). The ocean mass contribution is plotted on Figure 3b with estimations based on data from *Levitus et al*. [2012] (light blue curve) and from *Ishii and Kimoto* [2009] (dark blue curve). The land mass contribution is plotted on Figure 3c with estimations based on the LaD model (light green curve) and on the WGHM model (dark green curve). The sum of the ocean and land mass contributions to C_{20} is plotted on Figure 3d (black curve) with uncertainty (grey shaded area).

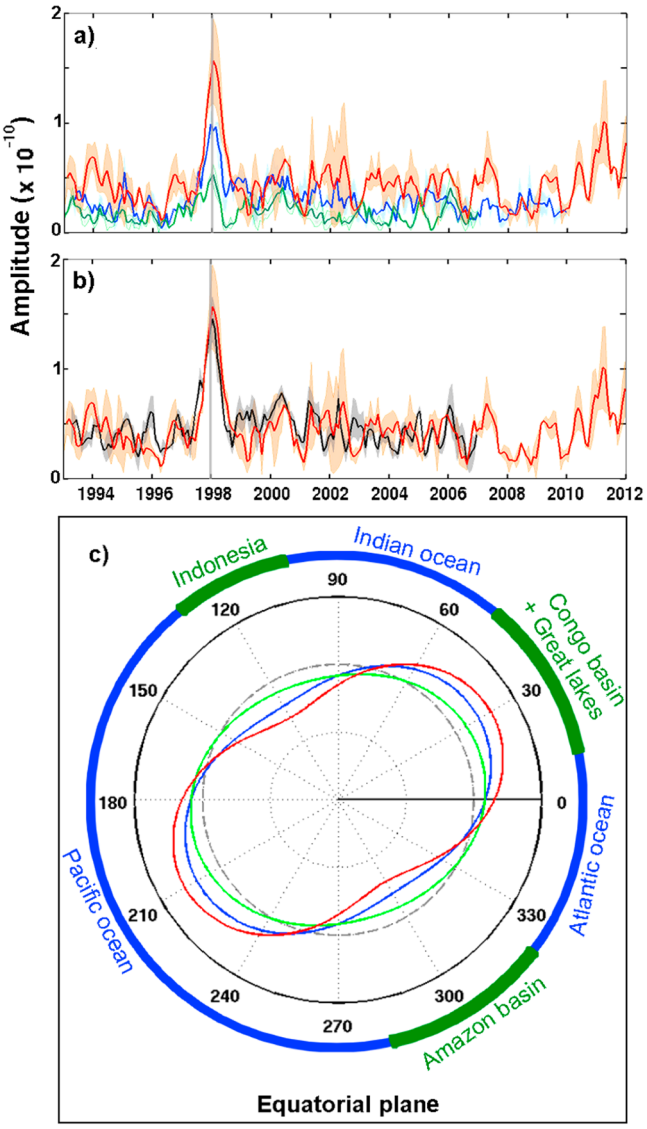

Figure 4. (a) Amplitude of the degree-2 order-2 spherical harmonics from SLR data (mean of CSR and GRGS solutions) (in red) with uncertainty (orange shaded area). The tropical ocean mass contribution and its uncertainty are plotted in blue. The land mass contribution and its uncertainty are plotted in green. (b) The sum of the tropical ocean and land mass contributions and their uncertainty are plotted in black. (c) Schematic plot of the equatorial projection of the degree-2 order-2 spherical harmonics in January 1998. The amplitude of the spherical harmonics has been amplified by a factor of 10^9 to facilitate the visualization while the phase has not been modified.

3. Results

3.1. $C_{2,2}$ and $S_{2,2}$ Variations

[10] Figure 1a shows estimates of detrended $S_{2,2}$ variations with the atmospheric effect removed, computed with the GRGS and CSR solutions from SLR data. Both estimates of GRGS and CSR agree well at interannual to decadal time scales. They show large interannual variations for $S_{2,2}$ (the standard deviation of the mean of both estimates is 0.48×10^{-10}) with a maximum during the 1997/1998 El Niño and a minimum during the 2011 La Niña. Ocean mass variations explain a large part of the interannual variations in $S_{2,2}$ (see Figure 1b). In particular, in 1998, about 70% of the total increase in $S_{2,2}$ is due to the ocean mass contribution. Variations in land water storage (hereafter LWS) also play a role in $S_{2,2}$ variations (see Figure 1c). But both hydrological models agree to show that the LWS contribution to $S_{2,2}$ interannual variations is rather small (with an amplitude lower than $\pm 0.3 \times 10^{-10}$) except during the 1997/1998 El Niño where it explains up to 30% of the total increase in $S_{2,2}$.

[11] From the GRGS-based and the CSR-based observed $S_{2,2}$, we compute an average $S_{2,2}$ and its related uncertainty (which is computed as the difference between the GRGS and CSR solutions). The same is done for the ocean mass contribution (from both estimations based on *Ishii and Kimoto* [2009] and *Levitus et al.* [2012]) and the LWS contribution (from both estimations based on WGHM and LaD). The mean LWS contribution from hydrological models combines well with the mean ocean mass contribution from altimetry corrected for the steric effect to explain the $S_{2,2}$ variations from SLR (see Figure 1d). In particular, the maximum in $S_{2,2}$ observed by SLR tracking data in 1998 during the 1997/1998 El Niño is well reproduced by the sum of the LWS and the ocean mass contributions. This is unlike the year 1999 during which the LWS and ocean mass contributions are seen to decrease very fast and are not sufficient to explain the $S_{2,2}$ variation observed by SLR tracking. The reason for this misfit in 1999 is not clear. It can be due to a lagged response of glaciers and small ice caps to the 1997/1998 El Niño. It could also be due to a contribution of the deep ocean since it is not taken into account in this study. But the latter option seems unlikely, given the long time response of the deep ocean to climate variability.

[12] There is less confidence in the variations of $C_{2,2}$ estimated from SLR tracking data than in $S_{2,2}$ variations because both estimates from GRGS and CSR show discrepancies as shown in Figure 2a. Indeed, GRGS and CSR $C_{2,2}$ time series show significant differences at interannual time scales even though they are fairly similar at decadal time scales until 2012. Ocean mass contribution to $C_{2,2}$ variations estimated from *Ishii and Kimoto* [2009] and *Levitus et al.* [2012] data sets also disagrees at interannual time scales except in 1998 (see Figure 2b). However, the LWS contributions estimated from WGHM and LaD is consistent over the whole period of study, since 1993 (see Figure 2c). As a result, $C_{2,2}$ variations estimated from SLR tracking data and the combination of ocean mass and LWS contributions are quite different. Nevertheless, we note that both estimations agree on showing small $C_{2,2}$ variations (0.37×10^{-10} of standard deviation for the SLR estimate and 0.32×10^{-10} for the sum of the ocean mass contribution and the LWS contribution). These $C_{2,2}$ variations are significantly smaller than the $S_{2,2}$ variations.

3.2. $C_{2,0}$ Variations

[13] Figure 3a shows $C_{2,0}$ variations with the atmospheric effects removed, estimated by GRGS and CSR from SLR data. Both estimates from GRGS and CSR are in very good agreement (within the formal error). They show large variations in $C_{2,0}$ (the standard deviation of the mean of both estimates is 0.42×10^{-10}) which reveal important interannual mass transfers between the tropics and the extratropics (in agreement with *Cox and Chao* [2002], *Dickey et al.* [2002], *Chen et al.* [2005], *Marcus et al.* [2009], and

Cheng and Tapley [2004], *Cheng et al*. [2013]). Variations in $C_{2,0}$ correlate well with the scaled Pacific Decadal Oscillation (PDO) index (a proxy of the low-frequency variability dominating the Pacific Ocean [*Zhang et al*., 1997]). This result confirms the result from *Chao et al*. [2003]. It indicates that the interannual latitudinal mass transfers between the tropics and the extratropics are of climatic origin and related to a natural climate mode of variability: the Pacific Decadal Oscillation. Ocean mass contribution to $C_{2,0}$ variations estimated from *Ishii and Kimoto* [2009] and *Levitus et al*. [2012] data sets is consistent (see Figure 3b). Both estimates show a fairly low ocean mass contribution to $C_{2,0}$ variations except in 1998. Estimations of the LWS contribution to $C_{2,0}$ variations from WGHM and LaD are also consistent (see Figure 3c). But unlike the ocean mass contribution, they show an important role of LWS on $C_{2,0}$ variations over the whole record. When combined together, the ocean mass contribution plus the LWS contribution to $C_{2,0}$ variations fit well the $C_{2,0}$ curve obtained from SLR data (see Figure 3d) (in agreement with previous studies that were based on models for the ocean contribution estimates like *Dickey et al*. [2002], *Chen et al*. [2005], *Chao et al*. [2003], and *Cheng et al*. [2004, 2013]). This shows that most of the interannual variability in $C_{2,0}$ variations are the result of changes in ocean mass, LWS, and atmospheric mass of climatic origin.

3.3. The 1997/1998 El Niño

[14] $C_{2,0}$ variations, whether they are estimated from SLR tracking data or the combination of ocean mass and LWS contributions, show a strong decrease during the 1997/1998 El Niño (between January 1997 and January 1999, see Figure 3d, see also *Cheng et al*. [2013]). This decrease reveals a sudden large mass transfer from high latitudes (>35.3°) to low latitudes (<35.3°) which lasted 2 years or so. Both ocean and land played a role in this latitudinal mass transfer but at different periods (confirming the qualitative analysis of *Marcus et al*. [2009]). Between January 1997 and December 1997, the latitudinal mass transfer was essentially due to ocean mass redistribution from high to low latitudes (see the decrease in ocean contribution to $C_{2,0}$ between January 1997 and December 1997 in Figure 3b), whereas between January 1998 and December 1998, the latitudinal mass transfer is rather seen in the LWS contribution to the $C_{2,0}$ variations (see Figure 3c).

[15] During the 2 year period, from January 1997 to December 1998, we can also observe an anticorrelation between the ocean mass contribution and the LWS contribution to $C_{2,0}$. The ocean mass contribution decreases over the period January 1997 to December 1997 while the LWS contribution slightly increases and vice versa over the period January 1998 to December 1998. This anticorrelation suggests that some important mass transfers between ocean and land at the same latitude also occurred during the 1997/1998 El Niño. This is confirmed when we look at the variations of the degree-2 order-2 spherical harmonic (which is related to longitudinal mass transfers) between January 1997 and December 1998. Figure 4 shows the degree-2 order-2 spherical harmonic coefficients variations around 1998. But instead of showing them in terms of $C_{2,2}$ and $S_{2,2}$ variations as in Figures 1 and 2, Figure 4 shows the amplitude ($\sqrt{C_{2,2}^2 + S_{2,2}^2}$) and the phase ($arctan\left(\frac{S_{2,2}}{C_{2,2}}\right)$) of the degree-2 order-2 spherical harmonic in 1998. The large amplitude observed in 1998 confirms that a large longitudinal mass redistribution occurred during the 1997/1998 El Niño (see the red curve on Figure 4). This longitudinal mass transfer is essentially due to longitudinal mass transfers within the tropics (between 30°S and 30°N, see the black curve on Figure 4). Both tropical ocean and tropical land contributions played a significant role in this global mass transfer: 70% of the mass transfer comes from the tropical ocean mass contribution and 30% comes from the tropical LWS contribution. The phase of the tropical LWS contribution reveals an increase of water mass in the Congo Basin and a decrease of water mass in the Amazon Basin during the 1997/1998 El Niño (see Figure 4b). This is consistent with independent estimations of the LWS in these basins in 1998 from *Llovel et al*. [2011]. The phase of the tropical ocean mass contribution reveals an increase of mass in the tropical Pacific Ocean which is consistent with the recent study of *Cazenave et al*. [2012] on ocean mass redistributions during the 1997/1998 El Niño.

4. Conclusion

[16] The observed variations in $C_{2,0}$, $C_{2,2}$, and $S_{2,2}$ from SLR data since 1993 provide a clear indication of interannual to decadal large-scale latitudinal and longitudinal mass redistributions within the Earth's system. Comparison of independent estimations of the ocean mass and the land water storage contributions to $C_{2,0}$, $C_{2,2}$, and $S_{2,2}$ variations corrected for the atmospheric effects shows that these mass transfers occur at the Earth's surface and are due to climate variability. In particular, during the 1997/1998 El Niño, $C_{2,0}$, $C_{2,2}$, and $S_{2,2}$ variations reveal a mass increase in the tropics and mass transfers between ocean and land within the tropics. These results are consistent with independent estimations of mass transfers over the period 1997–1998 from the literature. It confirms that SLR-derived estimates of the low-degree spherical harmonics of the Earth's gravity field can provide important information and constraints on the amplitude and the spatial structure of mass redistributions of climatic origin in the Earth's system.

[17] **Acknowledgments.** This work was supported by the Centre National d'Etudes Spatiales (CNES). The CSR time series was produced by NASA's MEaSUREs program under JPL contract. M.K. Cheng is supported by NASA grant NNX12AK13G. The altimeter products used here were produced by Ssalto/Duacs and distributed by AVISO with support from CNES.

[18] The Editor thanks two anonymous reviewers for their assistance in evaluating this paper.

References

Boening, C., J. K. Willis, F. W. Landerer, R. S. Nerem, J. Fasullo (2012), The 2011 La Niña: So strong, the oceans fell, *Geophys. Res. Lett.*, *39*, L19602, doi:10.1029/2012GL053055.

Cazenave, A., O. Henry, S. Munier, T. Delcroix, A. L. Gordon, B. Meyssignac, W. Llovel, H. Palanisamy, and M. Becker (2012), Estimating ENSO influence on the global mean sea level 1993–2010, *Mar. Geod.*, *35*, 82–97, doi:10.1080/01490419.2012.718209.

Chao, B. F., A. Y. Au, J. P. Boy, and C. M. Cox (2003), Time-variable gravity signal of an anomalous redistribution of water mass in the extratropic Pacific during 1998–2002, *Geochem. Geophys. Geosyst.*, *4*(11), 1096, doi:10.1029/2003GC000589.

Chen, J. L., C. R. Wilson, and B. D. Tapley (2005), Interannual variability of low-degree gravitational change, 1980–2002, *J. Geodes.*, *78*, 535–543, doi:10.1007/s00190-004-0417-y.

Cheng, M., B. D. Tapley, and J. C. Ries (2013), Deceleration in the Earth's oblateness, *J. Geophys. Res. Solid Earth*, *118*, 1–8, doi:10.1002/jgrb.50058.

Cheng, M. K., and B. D. Tapley (2004), Variations in the Earth's oblateness during the past 28 years, *J. Geophys. Res.*, *109*, B09402, doi:10.1029/2004JB003028.

Cox, C., and B. F. Chao (2002), Detection of large-scale mass redistribution in the terrestrial system since 1998, *Science*, *297*, 831 pp.

Desai, S. D. (2002), Observing the pole tide with satellite altimetry, *J. Geophys. Res.*, *107*(C11), 3186, doi:10.1029/2001JC001224.

Dickey, J. O., S. L. Marcus, O. de Viron, and I. Fukumori (2002), Recent Earth oblateness variations: Unraveling climate and postglacial rebound effects, *Science*, *298*(5600), 1975–1977, doi:10.1126/science.1077777.

Doll, P., F. Kaspar, and B. Lehner (2003), A global hydrological model for deriving water availability indicators: Model tuning and validation, *J. Hydrol.*, *270*(1–2), 105–134, doi:10.1016/S0022-1694(02)00283-4.

Forste, C., et al. (2008), The GeoForschungsZentrum Potsdam/Groupe de Recherche en Géodésie Spatiale satellite-only and combined gravity field models: EIGEN-GL04S1 and EIGEN-GL04C, *J. Geodes.*, *82*(6), 331–346, doi:10.1007/s00190-007-0183-8.

Gu, G., and R. F. Adler (2011), Precipitation and temperature variations on the interannual time scale: Assessing the impact of ENSO and volcanic eruptions, *J. Climate*, *24*(9), 2258–2270, doi:10.1175/2010JCLI3727.1.

Ishii, M., and M. Kimoto (2009), Reevaluation of historical ocean heat content variations with time-varying XBT and MBT depth bias corrections, *J. Oceanogr.*, *65*(3), 287–299, doi:10.1007/s10872-009-0027-7.

Levitus, S., et al. (2012), World ocean heat content and thermosteric sea level change (0–2000 m), 1955–2010, *Geophys. Res. Lett.*, *39*, L10603, doi:10.1029/2012GL051106.

Llovel, W., M. Becker, A. Cazenave, S. Jevrejeva, R. Alkama, B. Decharme, H. Douville, M. Ablain, and B. Beckley (2011), Terrestrial waters and sea level variations on interannual time scale, *Global Planet. Change*, *75*(1–2), 76–82, doi:10.1016/j.gloplacha.2010.10.008.

Lyard, F., F. Lefevre, T. Letellier, and O. Francis (2006), Modelling the global ocean tides: Modern insights from FES2004, *Ocean Dynam.*, *56*(5–6), 394–415, doi:10.1007/s10236-006-0086-x.

Marcus, S. L., J. O. Dickey, J. K. Willis, and F. Seitz (2009), Earth oblateness changes reveal land ice contribution to interannual sea level variability, *Geophys. Res. Lett.*, *36*, 23, doi:10.1029/2009GL041130.

Milly, P. C. D., and A. B. Shmakin (2002), Global modeling of land water and energy balances. Part I: The land dynamics (LaD) model, *J. Hydrometeorol.*, *3*(3), 283–299, doi:10.1175/1525-7541(2002)003<0283:GMOLWA>2.0.CO;2.

Nerem, R. S., and J. Wahr (2011), Recent changes in the Earth's oblateness driven by Greenland and Antarctic ice mass loss, *Geophys. Res. Lett.*, *38*, L13501, doi:10.1029/2011GL047879.

Pavlis, N. K., S. A. Holmes, S. C. Kenyon, and J. K. Factor (2012), The development and evaluation of the Earth Gravitational Model 2008 (EGM2008), *J. Geophys. Res.*, *117*, 2633, doi:10.1029/2011JB008916.

Pearlman, M. R., J. J. Degnan, and J. M. Bosworth (2002), "The International Laser Ranging Service", *Advances in Space Research*, *30*(2), pp. 135–143, doi:10.1016/S0273-1177(02)00277-6.

Roy, K., and W. R. Peltier (2011), GRACE era secular trends in Earth rotation parameters: A global scale impact of the global warming process?, *Geophys. Res. Lett.*, *38*, L10306, doi:10.1029/2011GL047282.

Syed, T. H., J. S. Famiglietti, and D. P. Chambers (2009), GRACE-based estimates of terrestrial freshwater discharge from basin to continental scales, *J. Hydrometeorol.*, *10*(1), 22–40, doi:10.1175/2008JHM993.1.

Zhang, Y., J. M. Wallace, and D. S. Battisti (1997), ENSO-like interdecadal variability: 1900–93, *J. Climate*, *10*, 1004–1020, doi:10.1175/1520-0442(1997)010<1004:ELIV>2.0.CO;2.